

# A NUMERICAL METHOD FOR A NONLOCAL FORM OF RICHARDS' EQUATION BASED ON PERIDYNAMIC THEORY

MARCO BERARDI, FABIO V. DIFONZO, AND SABRINA F. PELLEGRINO

ABSTRACT. Forecasting water content dynamics in heterogeneous porous media has significant interest in hydrological applications; in particular, the treatment of infiltration when in presence of cracks and fractures can be accomplished resorting to peridynamic theory, which allows a proper modeling of non localities in space. In this framework, we make use of Chebyshev transform on the diffusive component of the equation and then we integrate forward in time using an explicit method. We prove that the proposed spectral numerical scheme provides a solution converging to the unique solution in some appropriate Sobolev space. We finally exemplify on several different soils, also considering a sink term representing the root water uptake.

## 1. INTRODUCTION

Environmental protection and related sustainability management policies demand a thorough understanding of complex coupling between hydrology, soil sciences, ecology, agronomy, atmospheric sciences, calling for deeper mathematical modeling and numerical methods able to deal with the multiphysics processes involved in these environmental phenomena. In particular, flow processes in unsaturated media have to be studied for a better understanding of the whole water cycle; a correct managing of irrigation needs relies, for instance, on robust numerical solvers for unsaturated flows with root water uptake (see for instance, [24, 48]), or it is the basis for forecasting contaminant transport in the vadose zone (see for instance [55]). Classical local advection-diffusion equations in porous media often fail to describe accurately such complex phenomena.

The idea of incorporating non-local behaviors in standard unsaturated flow models is gaining interest in recent times. Besides non-localities in space, which are the focus of this paper, also non-local effects in time can be considered, that generally account for memory terms in the advection-diffusion equations: in some pioneering works in the early '60s [47]) it had been already noticed that diffusivity depends not only on water content, but also explicitly on time, and this argument has been then extended also to hydraulic conductivity (see [26]; later on a model, in which derivative of water content on time is fractional, has been first proposed in [44] and then generalized in [31]. A memory component has been observed also when modeling water stress in the root water uptake: the experimental evidence of such "ecological memory" of plant roots has been noticed, for instance, in [52, 14] and has been recently formalized in [7].

---

2020 *Mathematics Subject Classification.* 65M70, 42B30.

*Key words and phrases.* Richards' equation, Peridynamic, Nonlocal Model, Spectral Numerical Method.

When dealing with spatial discontinuities or significant heterogeneities, classical local formulations of flow and transport phenomena present severe limitations; for instance, in some cases, standard unsaturated flow models can not forecast correctly water dynamics; as reported in [42], when modeling fast infiltration processes (for instance infiltration after a heavy rainfall event), "first arrival time at the groundwater [...] are often under-predicted" because of preferential flow paths. These preferential flows can be ascribed to non-equilibrium of water pressure at a local scale. As a matter of facts, there is an experimental evidence that pore structures in natural soils dynamically change due to alternating swelling and shrinkage processes (see for instance [19]): this phenomenon can be described by a dual permeability approach, by which the bulk porous medium consists of two dynamic interacting pore domains: (i) the fracture (from shrinkage) pore domain and (ii) the aggregate (interparticles plus structural pores), respectively (see [20]): in practice, two different unsaturated flow equations are considered in each part of this domain. Analogously, in the context of solute transport, the solute exchange between mobile and immobile water has been modeled by a delay term in [39], and, in a computational framework, this approach has been implemented in [41].

More in detail, multirate mass transfer is modeled assuming advection-diffusion on the fast mobile continuum and only diffusion in the slow immobile continuum: after solving analytically the diffusion model, the consequent fast domain model results non-local in time ([15]). In this dual-continuum framework, the pioneering work [42] shows that the linearization of the nonlinear diffusion equation, governing capillary flow in the slow continuum, ensures a good description of the averaged water content dynamics in the slow domain: therefore, they derive a non-local Richards' equation in the mobile domain, endowed with a memory kernel encoding mass transfer dynamics of the slow domains.

From the viewpoint of applications, in this context, desiccation cracks impact the efficiency of irrigation and provokes a fast leakage of nutrients and contaminants below the root zone into the groundwater. Even worst is the effect of such cracks into an earth dam, since it may lead to the failure of the dam itself.

On the other hand, several efforts have been accomplished towards a comprehensive modeling and efficient numerical solvers for such nonlocal problems. In [53] the coupling of peridynamic formulation of chemical transport with water flow is proposed in the unsaturated context, and an implicit numerical solver is implemented, and tested over different case studies, in order to show the ability of the model to recognize discontinuities and heterogeneities, including stationary cracks, propagating cracks, and randomly distributed permeable and impermeable inclusions. In [22] authors discuss how a single continuum model can properly catch the contributions from all the flow paths only if the control volume (i.e. the computational cell) is much larger than the longest connections between pores: therefore a non-local model is proposed therein, showing that if the longest connections are much smaller than the size of the control volume, these models converge to Darcy's law. Nonlocal models and peridynamics are largely used in several context in order to model a more regular behavior of the solution, (see [45, 21, 18]). In particular, a significant work has been presented in [43], in which the peridynamic theory is employed for simulating hydraulic fracture propagation in saturated porous media, and it is coupled with FEM for forecasting fluid flow

therein. In this paper we aim at introducing a tailored numerical method for the corresponding peridynamic model of Richards' equation describing the unsaturated flow; more recently, in [49], an implicit peridynamic framework is devised for the solution of quasi-static problems involving brittle and quasi-brittle fracture. For the sake of clarity we should say that peridynamic theory was introduced by Silling in [50] as a nonlocal version of elasticity theory, for modeling long-range interactions occurring in real materials, ruling several phenomena like fractures, instabilities and cracks. In general, peridynamic models consist of an integro-differential equation not involving spatial derivatives and describe the motion of a material body subjected to external loading conditions. The theory prescribes the existence of a domain influence, called horizon, which represents a measure of the nonlocality of the model and defines the range of interactions between material particles.

In this framework, the remaining of the paper is structured as follows. In Section 2 an introduction to nonlocal framework and a peridynamic formulation of Richards' equation is given, with all the necessary assumptions to justify the current setting. Then, in Section 3, we propose a numerical method to integrate forward in time a semi-discretized version of the equation, leveraging spectral theory and Chebyshev transform properties to prove convergence results of the discretized solution to the exact one. The implementation of Chebyshev collocation method provides a good accuracy and does not require to impose periodic boundary conditions. Finally, in Section 4 we exemplify on different soils with several type of Dirichlet boundary conditions to support our findings.

**1.1. A short overview on Richards' equation.** It is well known that Richards' equation is a mass conservation law in terms of the volumetric moisture content  $\theta$  and of the soil matric head  $h_m$  defined on some compact domain  $\Omega \subseteq \mathbb{R}^3$ , coupled with the Buckingham-Darcy's law for the description on the flux:

$$\begin{aligned} \frac{\partial \theta}{\partial t}(\mathbf{x}, t) &= -\nabla q(\mathbf{x}, t) + S(\mathbf{x}, t, \theta), \quad \mathbf{x} \in \Omega \\ q(\mathbf{x}, t) &= -K(h_m)\nabla(h_m - z), \end{aligned}$$

where  $z$  is the elevation component of the space variable  $\mathbf{x}$ ,  $\theta$  represents the volumetric water content,  $K$  is the so called hydraulic conductivity and  $S(\mathbf{x}, t, \theta)$  is a source or sink term describing, for instance, the root water uptake. Thus, Richards' equation reads as

$$(1.1) \quad \frac{\partial \theta}{\partial t}(\mathbf{x}, t) - \nabla(K(h_m)\nabla(h_m - z)) = S(\mathbf{x}, t, \theta), \quad \mathbf{x} \in \Omega, t \in [0, T],$$

endowed with suitable initial and boundary conditions.

With the hypothesis that air pressure in the pores is constant, Richards' equation assumes that matric head at a given location is in equilibrium and that there exists a bijective function relating  $\theta$  with  $h_m$ , called water retention curve (see [42]), which is generally defined according to empirical functions. Moreover, for Richards' equation to be well posed,  $K$  must be smooth enough to guarantee existence and uniqueness of solutions, also in case of heterogeneous soils with smooth boundary (see [9] and references therein). In particular, hereafter and through the whole paper,  $K$  and  $h_m$  will be assumed to be locally Lipschitz on their respective domains; as a consequence, they are square integrable.

However, in case of desiccation cracks or anisotropic soils could affect well-posedness of Richards' equation (1.1) and prevent existence of any solution. An alternative approach has been proposed in [29], where theory of elasticity for solid mechanics has been applied to unsaturated, heterogeneous, anisotropic soils. In this case, though, the flow density function depends on the position, matric head or moisture content, instead of the relative distance and relative displacement [50, 51].

The numerous numerical issues arising when solving Richards' equation in a computational framework rely mainly in its nature of highly nonlinear degenerate elliptic parabolic PDE. Here we just mention some significant references for the main numerical problems arising in Richards' equation. For instance, since implicit methods are generally used for time integration, the arising nonlinear problems have been studied with different methods, such as Newton's (e.g. [16, 11], Picard ([17]), L-Scheme or its variants ([46, 40]). Even richer is the literature on spatial discretization techniques, for which we refer to [3, 33, 38, 32] and references therein. Approaches based on the transversal method of lines are adopted, with different goals and with different scopes, in [6, 5, 10].

In this paper, we are looking at the 1D version of (1.1) equipped with initial and Dirichlet boundary conditions, so that  $\Omega = [0, Z]$  for some  $Z > 0$ , and the forcing term  $S$  only depends on  $z \in [0, Z]$ . Thus, one considers

$$(1.2) \quad \frac{\partial \theta}{\partial t}(z, t) - \frac{\partial}{\partial z} \left( K(h_m) \frac{\partial}{\partial z} (h_m - z) \right) = S(z), \quad z \in [0, Z], t \in [0, T].$$

## 2. PERIDYNAMIC MODEL: ASSUMPTIONS AND DERIVATION

Since we are focusing on the 1D case, let us consider a compact interval  $\Omega = [0, Z]$  and let us define

$$(2.1) \quad B_\delta(z) := \{z' \in \Omega : |z' - z| \leq \delta\},$$

the *horizon* of  $z$  of radius  $\delta > 0$ . We assume that moisture dynamics at  $z$  is only affected by pairwise interaction with  $z' \in B_\delta(z)$ ; points outside the horizon of  $z$  do not contribute to any dynamics therein.

The model is built on the concept of peripipes. Given any  $z \in \Omega$ , we assume that for each  $z' \in B_\delta(z)$  there exists a fictitious pipe, called *peripipe*, connecting every  $z$  to  $z'$ . We assume that the following requirements hold for any peripipe (see [28]):

- (1) Moisture is stored at the endpoints  $z, z'$  of a peripipe, and zero moisture content is located along a peripipe;
- (2) moisture flows in the direction of the peripipe and no transversal flux crosses its boundaries
- (3) a peripipe is purely resistive, it has zero reactance and its response is proportional to the difference of the total hydraulic potential (see below)  $H(z) - H(z')$ ;
- (4) a peripipe has uniform conductivity;
- (5) peripipe conductivity is function of medium conductivity at its endpoints;
- (6) the length of a peripipe is  $|z - z'|$ ;
- (7) peripipe response may also depend on its length.

Following [29] and requirements above, we assume that the rate of volumetric moisture flow from a point  $z'$  to a point  $z$  per unit volume of  $z$  and per unit volume of  $z'$  is

given by

$$(2.2) \quad J(z, z', t) = C(z, z')(H(z', t) - H(z, t)),$$

where  $C(z, z')$  is the peridynamic hydraulic conductance density and  $H(z, t)$  is the total hydraulic potential, defined as

$$H(z, t) = h_m(z, t) + z.$$

Hereafter, for the sake of readability, we omit time dependence, unless required by the context.

The peripipe conductance depends on the peridynamic hydraulic conductivity  $\kappa(z', z)$ , which is an intrinsic material property (related to the classical hydraulic conductivity  $K$ ), in the following way:

$$(2.3) \quad C(z, z') = \frac{\kappa(z', z)}{|z - z'|},$$

where

$$(2.4) \quad \kappa(z, z') := K\varphi(z - z').$$

The function  $\varphi(z - z')$  is the so-called *influence function*, representing a convolution kernel relating the horizon (2.1) with the nature of boundary conditions assigned to (1.2). The shape of such an even function and the way to select it turns out to be crucial, as we will see in Section 2.1.

Therefore, the changes of moisture stored at  $z$  and at  $z'$ , mediated by the peripipe  $zz'$ , are given by

$$\begin{aligned} \Delta J(z, z') &= \kappa(z', z) \frac{H(z') - H(z)}{|z - z'|} dz' dz, \\ \Delta J(z', z) &= \kappa(z, z') \frac{H(z) - H(z')}{|z' - z|} dz dz'. \end{aligned}$$

As an immediate consequence it must hold  $\kappa(z, z') = \kappa(z', z)$ .

In case of non-homogeneous soils in unsaturated regime, the relations above could be leveraged to define a peridynamic conductivity density by setting

$$(2.5) \quad \kappa(z, z') := \frac{\kappa(z) + \kappa(z')}{2},$$

where  $\kappa(z) \equiv \kappa(z, 0)$ , as proposed in [53, 29].

Now, since the change over time of volumetric moisture content due to  $z'$  at time  $t$ , on the account of (2.2), is given by

$$\frac{\partial \theta}{\partial t}(z|z', t) = J(z, z'),$$

from which

$$\frac{\partial \theta}{\partial t}(z, t) = \int_{B_\delta(z)} J(z, z') dz' + S(z).$$

Thus, using (2.3) and with peridynamic conductivity given by (2.5), our model (1.2), endowed with Dirichlet boundary conditions, reads

$$(2.6a) \quad \frac{\partial \theta}{\partial t} = \int_{B_\delta(z)} \frac{\varphi(z' - z)}{|z' - z|} \frac{K(z) + K(z')}{2} [H(z') - H(z)] dz' + S(z),$$

$$(2.6b) \quad \theta(z, 0) = \theta^0(z), \quad z \in [0, Z],$$

$$(2.6c) \quad \theta(0, t) = \theta_0(t), \quad t \in [0, T],$$

$$(2.6d) \quad \theta(Z, t) = \theta_Z(t), \quad t \in [0, T].$$

**citare** [49]

**2.1. Selection of the influence function.** Usually (see, e.g. [53, 12, 29])  $\varphi(z)$  in (2.4) represents a convolution kernel, which can be chosen as a uniform influence function

$$\varphi(z) := \begin{cases} \frac{2}{\delta}, & |z| \leq \delta, \\ 0, & |z| > \delta, \end{cases}$$

or as a linear influence function

$$\varphi(z) := \begin{cases} 1 - \frac{|z|}{\delta}, & |z| \leq \delta, \\ 0, & |z| > \delta. \end{cases}$$

However, since such kernels would suggest the model to weigh more those cells where they are nonzero, and since our boundary conditions would typically be of Dirichlet type, we propose to consider a *distributed influence function* (see Figure 1), concentrated on the horizon boundary, of the form

$$(2.7) \quad \varphi_\delta(z) := \begin{cases} \frac{|z|-1+\delta}{\delta}, & |z| \geq 1 - \delta, \\ 0, & |z| < 1 - \delta. \end{cases}$$

In so doing, we are suggesting the model to averaging out not just what happens in the middle of the dynamics, but rather the behavior around each point of the spatial domain. Thus, specifically on the domain boundary, such a choice provides a nonlocal interaction with boundary conditions. Indeed, our aim is to avoid local Dirichlet boundary conditions in favor of nonlocal Dirichlet boundary conditions, that seem to be more appropriate in the peridynamic context, as showed in [2, 54]. Moreover, as we will see in Proposition 3.5, using (2.7) turns out to be crucial for the boundedness of the peridynamic operator, which is necessary to prove convergence of the numerical scheme to the unique solution to (2.6). In all our experiments, presented in Section 4, uniform and linear influence functions do not make our proposed numerical method converge, resulting in instabilities and blow-ups after a relatively small amount of time integration; on the other hand, and as presented below, using (2.7) guarantees stability and convergence, plus a reasonable shape of the numerical solutions.

### 3. NUMERICAL METHOD

The nonlocal Richards' equation (2.6) can be discretized in space by using Chebyshev polynomials. This approach is typically used when the integral operator can be expressed in terms of convolution products [35, 34, 37]. Moreover, the choice of such

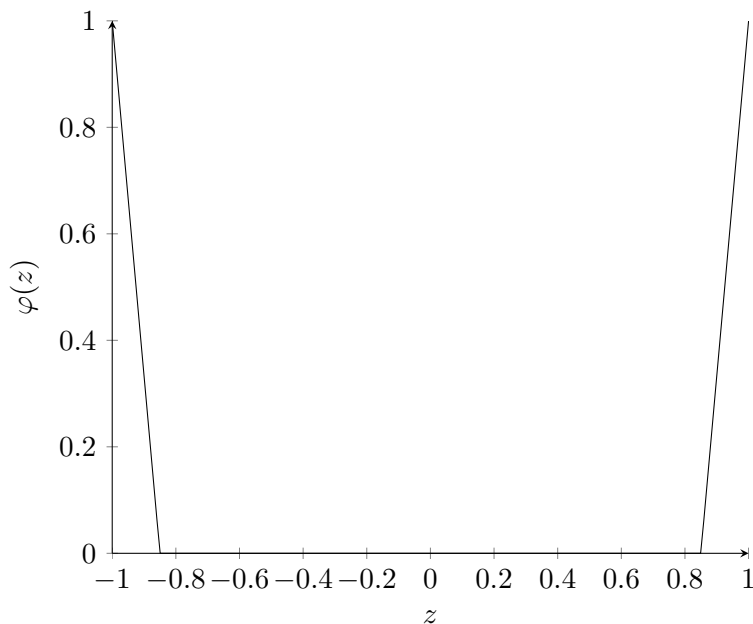


FIGURE 1. Distributed influence function defined in (1) with  $\delta = 0.15$ .

kind of polynomials allows us to overcome the limitation of imposing periodic boundary condition, which is necessary when dealing with Fourier trigonometric polynomials.

The proposed technique consists in looking for an approximation of  $\theta(x, t)$  in the form of a finite linear combination of Chebyshev polynomials of the first kind. To do so, we can assume the spatial domain to be  $[-1, 1]$ , as we can benefit of the orthogonality properties of the polynomials. However, a more general interval can be used as spatial domain by linearity. Moreover, for time integration we use the explicit Euler method, as in [53].

In this section we briefly make a review on Chebyshev polynomials, then we derive the semidiscrete model of (2.6) and finally prove the convergence of the proposed method.

**3.1. Basic overview on Chebyshev polynomials.** Chebyshev polynomials of the first kind,  $T_k(z)$  are defined by

$$T_k(z) = \cos(k \arccos(z)), \quad z \in [-1, 1], \quad k \in \mathbb{N},$$

and are orthogonal with respect to the weight function  $w(z) := (\sqrt{1 - z^2})^{-1}$ .

These polynomials are commonly used in the context of spectral approximation because they satisfy an interpolation property: given an integer  $N$ , any sufficiently smooth function  $u$  defined on  $[-1, 1]$  can be expanded as an  $(N + 1)$ -term linear combination of polynomials  $u^N$  given by

$$(3.1) \quad u^N(z) := \sum_{k=0}^N \tilde{u}_k T_k(z),$$

where  $\tilde{u}_k$  are the coefficients of the expansion and approximate the Chebyshev coefficients

$$\hat{u}_k = \frac{2}{\pi c_k} \int_{-1}^1 u(z) T_k(z) w(z) dz,$$

with

$$c_k = \begin{cases} 2 & k = 0 \\ 1 & k \neq 0. \end{cases}$$

The explicit expression of  $\tilde{u}_k$  depends on the choice of the grid points used to discretize  $[-1, 1]$ . In particular, if we choose the Gauss-Lobatto collocation points

$$(3.2) \quad z_h := \cos\left(\frac{h\pi}{N}\right), \quad h = 0, \dots, N,$$

the expression of  $\tilde{u}_k$  is

$$(3.3) \quad \tilde{u}_k = \frac{1}{\gamma_k} \sum_{h=0}^N u(z_h) T_k(z_h) w_h,$$

where  $\gamma_k$  is a normalization constant defined by

$$(3.4) \quad \gamma_k := \begin{cases} \pi & k = 0, N \\ \frac{\pi}{2} & k = 1, \dots, N-1 \end{cases}$$

and

$$(3.5) \quad w_h := \begin{cases} \frac{\pi}{2N} & h = 0, N \\ \frac{\pi}{N} & h = 1, \dots, N-1. \end{cases}$$

Equation (3.1) represents the inverse discrete Chebyshev transform, while the coefficients  $\tilde{u}_k$  in (3.3) correspond to the discrete Chebyshev transform. They can be efficiently computed using the Fast Fourier Transform. Additionally, they fulfill the same properties of the Fourier transform. In particular, we can rewrite a convolution product in the physic space as a multiplication of the Chebyshev transform of each factor in the frequency space.

The following result shows the rate of convergence of the Chebyshev approximation.

**Theorem 3.1** (see [13]). *For any  $0 \leq \mu \leq 2$  and  $u \in L^2([-1, 1])$ , there exists a positive constant  $C$  independent on  $N$ , such that*

$$(3.6) \quad \|u - u^N\|_{L^2([-1, 1])} \leq \frac{C}{N^{2-\mu}} \|u\|_{L^2([-1, 1])}.$$

In the next section, to lighten the notation, we denote the Chebyshev transform by  $\mathcal{F}$  and the inverse Chebyshev transform by  $\mathcal{F}^{-1}$ .

**3.2. Chebyshev semi-discrete collocation method for the nonlocal Richards' equation.** In what follows, we develop a spectral approximation of (2.6) by using the Chebyshev transform. We fix  $N > 0$  and assume  $\Omega = [-1, 1]$ . We can discretize the spatial domain by the Gauss-Lobatto points  $z_h$ ,  $h = 0, \dots, N$  defined in (3.2).



If we set

$$\begin{aligned}\Lambda(z) &:= K(z)H(z), \\ \bar{\varphi}_\delta(z) &:= \frac{\varphi_\delta(z)}{\|z\|}, \\ \beta &:= \int_{-1}^1 \bar{\varphi}_\delta(z) \, dz,\end{aligned}$$

then, since from distributed influence function definition (2.7) it follows that  $\beta = 2(1 + \frac{1-\delta}{\delta} \ln(1-\delta))$ , we can rewrite model (2.6a) as

$$\begin{aligned}(3.7) \quad \frac{\partial \theta}{\partial t} &= \int_{B_1(z)} \frac{\varphi_\delta(z' - z)}{\|z' - z\|} \frac{K(z') + K(z)}{2} [H(z') - H(z)] \, dV_{z'} + S(z), \\ &= \frac{1}{2} [(\bar{\varphi}_\delta * \Lambda)(z) + K(z)(\bar{\varphi}_\delta * H)(z) - H(z)(\bar{\varphi}_\delta * K)(z) - \beta \Lambda(z)] + S(z).\end{aligned}$$

Thus, the right hand side of (3.7) can be computed by means of the finite discrete Chebyshev transform. Indeed, we have

$$(3.8) \quad (\bar{\varphi}_\delta * \Lambda)(z) = \mathcal{F}^{-1}(\mathcal{F}(\bar{\varphi}_\delta) \mathcal{F}(\Lambda))(z),$$

$$(3.9) \quad (\bar{\varphi}_\delta * H)(z) = \mathcal{F}^{-1}(\mathcal{F}(\bar{\varphi}_\delta) \mathcal{F}(H))(z),$$

$$(3.10) \quad (\bar{\varphi}_\delta * K)(z) = \mathcal{F}^{-1}(\mathcal{F}(\bar{\varphi}_\delta) \mathcal{F}(K))(z).$$

So, at each collocation point  $z_h$ , the semi-discretization of the model reads

$$\begin{aligned}(3.11) \quad \frac{\partial \theta}{\partial t}(z_h, t) &= \frac{1}{2} (\mathcal{F}^{-1}(\mathcal{F}(\bar{\varphi}_\delta) \mathcal{F}(\Lambda))(z_h) + K(z_h) \mathcal{F}^{-1}(\mathcal{F}(\bar{\varphi}_\delta) \mathcal{F}(H))(z_h)) \\ &\quad - \frac{1}{2} (H(z_h) \mathcal{F}^{-1}(\mathcal{F}(\bar{\varphi}_\delta) \mathcal{F}(K))(z_h) + \beta \Lambda(z_h)) + S(z_h)\end{aligned}$$

The function  $\Lambda$  is defined as the product between the conductivity  $K$  and the hydraulic potential  $H$ : therefore, to compute its Chebyshev transform, we first need to compute a product. The computational cost to obtain this term could be efficiently reduced by observing that the Chebyshev coefficients of  $\Lambda$  can be obtained from the Chebyshev coefficients of  $H$  and  $K$ .

Indeed, the following result holds (see [4]).

**Theorem 3.2.** *Let  $N \in \mathbb{N}$ . If  $H$  and  $K$  are approximated by a finite series of Chebyshev polynomials  $H^N$  and  $K^N$ , respectively, given by*

$$H^N(z) = \sum_{j=0}^N \tilde{H}_j T_j(z), \quad K^N(z) = \sum_{j=0}^N \tilde{K}_j T_j(z),$$

then the product  $\Lambda(z) = H(z)K(z)$  can be approximated by the following  $2N + 1$  combination of Chebyshev polynomials

$$\Lambda^N(z) = \sum_{j=0}^{2N} \tilde{\Lambda}_j T_j(z),$$

where the coefficients  $\tilde{\Lambda}_j$  are given by

$$2\tilde{\Lambda}_j = \begin{cases} 2\tilde{H}_0\tilde{K}_0 + \sum_{\ell=1}^N \tilde{H}_\ell\tilde{K}_\ell, & j = 0 \\ \sum_{\ell=0}^j \tilde{H}_{j-\ell}\tilde{K}_\ell + \sum_{\ell=0}^{N-j} \tilde{H}_{j+\ell}\tilde{K}_\ell + \sum_{\ell=j}^N \tilde{H}_{\ell-j}\tilde{K}_\ell, & j = 1, \dots, N \\ \sum_{\ell=j-N}^N \tilde{H}_{j-\ell}\tilde{K}_\ell, & j = N+1, \dots, 2N. \end{cases}$$

The application of Theorem 3.2 implies that the first term in the right hand side of (3.11) is discretized by  $2N+1$  mesh points. Therefore, to maintain the consistency of the scheme, the discretization of the remaining terms on the right hand side of (3.11) is accomplished by considering  $2N+1$  Gauss-Lobatto collocation points.

**3.3. Convergence of the semi-discrete scheme.** We prove the convergence of the spectral semi-discrete method in a suitable weighted Hilbert space. Throughout this section,  $C$  denotes a generic constant.

We consider the weighted Lebesgue space

$$L_w^2([-1, 1]) = \left\{ u \in L^2 : \int_{-1}^1 u^2(z)w(z)dz < +\infty \right\}$$

equipped with the inner product and the norm respectively

$$(u, v)_w = \int_{-1}^1 u(z)v(z)w(z) dz, \quad \|u\|_w^2 = (u, u)_w,$$

where  $w(z) = (\sqrt{1-z^2})^{-1}$ .

For any  $s \geq 0$ , we set

$$H_w^s([-1, 1]) = \left\{ u \in L_w^2([-1, 1]) \mid \|u\|_{s,w} < +\infty \right\},$$

where

$$\|u\|_{s,w}^2 = \sum_{|\alpha| \leq s} \|D^\alpha u\|_w^2.$$

Let  $S_N$  be the space of Chebyshev polynomials of degree  $N$ ,

$$S_N := \text{span} \{T_h(x) \mid 0 \leq h \leq N\} \subset L_w^2([-1, 1]),$$

and  $P_N : L_w^2([-1, 1]) \rightarrow S_N$  be an orthogonal projection operator

$$P_N u(x) := \sum_{h=0}^N \hat{u}_h T_h(x) w_h,$$

for  $w_h$  defined in (3.5), such that for any  $u \in L_w^2([-1, 1])$ , the following equality holds

$$(3.12) \quad (u - P_N u, \varphi)_w = 0, \quad \text{for every } \varphi \in S_N.$$

The projection operator  $P_N$  commutes with derivatives in the distributional sense:

$$\partial_t^q P_N u = P_N \partial_t^q u, \quad q \in \mathbb{N}, q \geq 1,$$

where, as usual,  $\partial_t := \frac{\partial}{\partial t}$ .

Letting  $s \geq 1$ , we denote by  $X_s := C^0(0, T; H_w^s([-1, 1]))$  the space of all continuous functions in the weighted Sobolev space  $H_w^s([-1, 1])$ , with norm

$$\|u\|_{X_s}^2 := \max_{t \in [0, T]} \|u(\cdot, t)\|_{s,w}^2,$$

for any  $T > 0$ . We denote by  $\mathcal{L}$  the nonlocal integral operator of (2.6), namely

$$(3.13) \quad \mathcal{L}(\theta) := \int_{B_1(z)} \frac{\varphi_\delta(z' - z)}{\|z' - z\|} \frac{K(z) + K(z')}{2} [H(z') - H(z)] dV_{z'}.$$

Then, the semi-discrete spectral scheme for (2.6) can be rewritten as

$$(3.14) \quad \frac{\partial \theta^N}{\partial t} = P_N \mathcal{L}(\theta^N) + P_N S(z),$$

$$(3.15) \quad \theta^N(z, 0) = P_N \theta^0(z),$$

where  $\theta^N(z, t) \in S_N$  for every  $0 \leq t \leq T$ .

To obtain the convergence of the semi-discrete scheme, we need of the following lemma.

**Lemma 3.3** ([13, Theorem 3.1]). *For any real  $0 \leq \mu \leq s$ , there exists a positive constant  $C$  such that*

$$(3.16) \quad \|\theta - P_N \theta\|_{H_w^\mu([-1,1])} \leq \frac{C}{N^{s-\mu}} \|\theta\|_{H_w^s([-1,1])}, \quad \text{for every } \theta \in H_w^s([-1,1]).$$

Recalling that  $K$  and  $h_m$  are locally Lipschitz in their respective domains, we can prove the following theorem.

**Theorem 3.4.** *Let  $s \geq 1$  and  $\theta(z, t) \in X_s$  be the solution to the initial-boundary-valued problem (2.6) and  $\theta^N(z, t)$  be the solution to the semi-discrete scheme (3.14)-(3.15). Then, there exists a positive constant  $C$ , independent on  $N$ , such that*

$$(3.17) \quad \|\theta - \theta^N\|_{X_1} \leq C(T) \left(\frac{1}{N}\right)^{s-1} \|\theta\|_{X_s},$$

for any initial data  $\theta^0 \in H_w^s([-1,1])$  and for any  $T > 0$ .

*Proof.* Let  $s \geq 1$ . Using the triangular inequality, we have

$$(3.18) \quad \|\theta - \theta^N\|_{X_1} \leq \|\theta - P_N \theta\|_{X_1} + \|P_N \theta - \theta^N\|_{X_1}.$$

Lemma 3.3 implies

$$\|(\theta - P_N \theta)(\cdot, t)\|_{H_w^1([-1,1])} \leq \frac{C}{N^{s-1}} \|\theta(\cdot, t)\|_{H_w^s([-1,1])}.$$

Therefore,

$$(3.19) \quad \|\theta - P_N \theta\|_{X_1} \leq \frac{C}{N^{s-1}} \|\theta\|_{X_s}.$$

Subtracting (3.14) from (2.6) and taking the weighted inner product with  $P_N\theta - \theta^N \in S_N$ , we have

$$\begin{aligned}
(3.20) \quad 0 &= \underbrace{\int_{-1}^1 (\partial_t\theta(z,t) - \partial_t\theta^N(z,t)) (P_N\theta(z,t) - \theta^N(z,t)) w(z) dz}_{=:I_1} \\
&\quad - \underbrace{\int_{-1}^1 (\mathcal{L}(\theta(z,t)) - P_N\mathcal{L}(\theta^N(z,t))) (P_N\theta(z,t) - \theta^N(z,t)) w(z) dz}_{=:I_2} \\
&\quad - \underbrace{\int_{-1}^1 (S(z,t) - P_NS(z,t)) (P_N\theta(z,t) - \theta^N(z,t)) w(z) dz}_{=:I_3}.
\end{aligned}$$

The orthogonal condition (3.12) implies that

$$\int_{-1}^1 (\partial_t\theta(z,t) - P_N\partial_t\theta(z,t)) (P_N\theta(z,t) - \theta^N(z,t)) w(z) dz = 0,$$

and

$$\int_{-1}^1 (S(z) - P_NS(z)) (P_N\theta(z,t) - \theta^N(z,t)) w(z) dz = 0.$$

Thus,

$$\begin{aligned}
(3.21) \quad I_1 &= \int_{-1}^1 (\partial_t\theta(z,t) - P_N\partial_t\theta(z,t)) (P_N\theta(z,t) - \theta^N(z,t)) w(z) dz \\
&\quad + \int_{-1}^1 (P_N\partial_t\theta(z,t) - \partial_t\theta^N(z,t)) (P_N\theta(z,t) - \theta^N(z,t)) w(z) dz \\
&= \frac{1}{2} \frac{d}{dt} \|(P_N\theta - \theta^N)(\cdot, t)\|_{H_w^1([-1,1])}^2.
\end{aligned}$$

Since it is straightforward to see that  $I_3 = 0$ , we can focus on  $I_2$ . From (3.12) it follows that

$$\int_{-1}^1 (\mathcal{L}(\theta^N(z,t)) - P_N\mathcal{L}(\theta^N(z,t))) (P_N\theta(z,t) - \theta^N(z,t)) w(z) dz = 0,$$

and so, due to the locally Lipschitzianity of  $K$  and  $h_m$  and from Cauchy and triangular inequalities, we obtain

$$\begin{aligned}
(3.22) \quad I_2 &= \int_{-1}^1 (\mathcal{L}(\theta(z,t)) - \mathcal{L}(\theta^N(z,t))) (P_N\theta(z,t) - \theta^N(z,t)) w(z) dz \\
&\leq C \|(\theta - \theta^N)(\cdot, t)\|_{H_w^1([-1,1])}^2 + C \|(P_N\theta - \theta^N)(\cdot, t)\|_{H_w^1([-1,1])}^2 \\
&\leq 2C \|(\theta - P_N\theta)(\cdot, t)\|_{H_w^1([-1,1])}^2 + 3C \|(P_N\theta - \theta^N)(\cdot, t)\|_{H_w^1([-1,1])}^2,
\end{aligned}$$

where  $C > 0$  is a suitable selected constant. Plugging (3.21) and (3.22) in (3.20), we have

$$(3.23) \quad \frac{d}{dt} \|(P_N\theta - \theta^N)(\cdot, t)\|_{H_w^1([-1,1])}^2 \leq 4C \|(\theta - P_N\theta)(\cdot, t)\|_{H_w^1([-1,1])}^2 + 6C \|(P_N\theta - \theta^N)(\cdot, t)\|_{H_w^1([-1,1])}^2.$$

Since  $\|(P_N\theta - \theta^N)(\cdot, 0)\|_{H_w^1([-1,1])} = 0$ , Lemma 3.3 and Gronwall's inequality imply that

$$\begin{aligned} \|(P_N\theta - \theta^N)(\cdot, t)\|_{H^1([-1,1])}^2 &\leq 4C \int_0^t e^{6C(t-\tau)} \|(\theta - P_N\theta)(\cdot, \tau)\|_{H_w^1([-1,1])}^2 d\tau \\ &\leq \frac{C(T)}{N^{2s-2}} \int_0^t \|\theta(\cdot, \tau)\|_{H_w^1([-1,1])}^2 d\tau. \end{aligned}$$

Hence,

$$(3.24) \quad \|P_N\theta - \theta^N\|_{X_1} \leq \frac{C(T)}{N^{s-1}} \|\theta\|_{X_s}.$$

Finally, using (3.19) and (3.24) in (3.18), we complete the proof.  $\square$

**3.4. Fully-discrete scheme.** As already mentioned above, to integrate in time (2.6) we use the Forward Euler method. In fact, we widely experimented on using implicit methods for solving (3.7), all providing bad results, mainly depending - according to our experience - on the function  $K$ . Such negative results turned out to be independent on the influence functions selected.

From (3.11) and further considering initial conditions, the fully-discrete scheme writes as, for  $m = 0, \dots, N_T - 1$ ,  $h = 0, \dots, N$ ,

$$(3.25) \quad \begin{aligned} \theta_{m+1}(z_h) &= \theta_m(z_h) \\ &+ \Delta t \left( \frac{1}{2} (\mathcal{F}^{-1} (\mathcal{F}(\bar{\varphi}_\delta) \mathcal{F}(\Lambda)))(z_h) + K(z_h) \mathcal{F}^{-1} (\mathcal{F}(\bar{\varphi}_\delta) \mathcal{F}(H))(z_h) \right. \\ &\quad \left. - \frac{1}{2} (H(z_h) \mathcal{F}^{-1} (\mathcal{F}(\bar{\varphi}_\delta) \mathcal{F}(K)))(z_h) + \beta \Lambda(z_h) + S(z_h) \right), \end{aligned}$$

where  $\theta_m(z_h) = \theta(z_h, t_m)$ ,  $m = 0, \dots, N_T$ .

Therefore, the fully-discrete spectral scheme for (2.6) can be rewritten as

$$(3.26) \quad \theta_{m+1}^N = \theta_m^N + \Delta t (P_N \mathcal{L}(\theta_m^N) + P_N S(z)),$$

$$(3.27) \quad \theta_0^N(z) = P_N \theta_0^0(z),$$

where  $\theta_m^N(z) \in S_N$  for every  $m = 0, \dots, N_T$ .

The following result is preliminary for an error estimate of the fully discrete scheme (3.25), which is deferred to a forthcoming paper.

**Proposition 3.5.** *Let  $\theta_m^N(z)$  be the solution to the fully-discrete scheme (3.26)-(3.27). Then,  $\mathcal{L}(\theta_m^N) \in L^2([-1, 1])$ .*

*Proof.* Due to the definition of  $\varphi_\delta$  in (2.7) and since  $H$  and  $K$  are in  $L^2([-1, 1])$ , using the Cauchy-Schwartz inequality, we find

$$\int_{-1}^1 (\mathcal{L}(\theta_m^N))^2 dz = \int_{B_1(z)} \frac{(\varphi_\delta(z' - z))^2}{\|z' - z\|^2} \frac{(K(z) + K(z'))^2}{4} (H(z') - H(z))^2 dV_{z'} < \infty,$$

and this proves the claim.  $\square$

**Remark 3.6.** *We stress that, as a consequence of Proposition 3.5, in selecting spatial mesh for applying the numerical scheme (3.25), it will be guaranteed that no singularity will arise, no matter how we define collocation points.*

We then pose the following conjecture, that is supported by numerical results in Section 4.

**Conjecture 1.** *Let  $\theta(z, t)$  be the solution to the initial-boundary valued problem (2.6) and  $\theta_m^N(z)$  be the solution to the fully-discrete scheme (3.26)-(3.27). Then, there exists a positive constant  $C$ , independent on  $N, N_T$ , such that*

$$(3.28) \quad \|\theta(t_m) - \theta_m^N\|_{L^2([-1,1])} \leq C \left( \frac{1}{N^2} + \Delta t \right) \|\theta_0 - \theta_0^N\|_{L^2([-1,1])}$$

#### 4. NUMERICAL SIMULATIONS

In this section we test our proposed method on different soils, possibly with a sink forcing term, representing the water uptake due to root systems. Van Genuchten - Mualem constitutive relations are considered in the following numerical simulations. We consider the classical Van Genuchten-Mualem constitutive relations in the unsaturated zone, given by

$$\begin{aligned} \theta(h_m) &= \theta_r + \frac{\theta_S - \theta_r}{(1 + |\alpha h_m|^n)^m}, \quad m := 1 - \frac{1}{n}, \\ K(h_m) &= K_S \left[ \frac{1}{1 + |\alpha h_m|^n} \right]^{\frac{m}{2}} \left[ 1 - \left( 1 - \frac{1}{1 + |\alpha h_m|^n} \right)^m \right]^2, \end{aligned}$$

where  $\theta_r$  and  $\theta_S$  represent the residual and the saturated water content, respectively,  $K_S$  the saturated hydraulic conductivity, and  $\alpha, n$  are fitting parameters.

**Example 4.1.** *As in [27], we consider a Berino loamy fine sand, with parameters*

$$\theta_r = 0.0286, \theta_S = 0.3658, \alpha = 0.0280, n = 2.2390, K_S = 0.0063 \text{ cm/s.}$$

*We added a sink term  $S = -100 \text{ s}^{-1}$  and parameter  $\delta = 0.15$  in (2.1). We set our initial and boundary conditions as follows*

$$\begin{aligned} \theta(0, t) &= 0.3 \left( 1 - \frac{t}{T} \right) + 0.29 \frac{t}{T}, \quad t \in [0, T], \\ \theta(Z, t) &= 0.2, \quad t \in [0, T], \end{aligned}$$

*while initial condition has a nonlinear profile*

$$\theta(z, 0) = 0.05x^3 + 0.25, \quad x := \frac{Z - 2z}{Z}, \quad z \in [0, Z].$$

*We select  $Z = 70 \text{ cm}$ ,  $T = 600 \text{ s}$ ; moreover, we used  $\Delta t = 0.06 \text{ s}$  and  $\Delta x = 0.3 \text{ cm}$ . Results are shown in Figure 2.*

*For this example, we report about the convergence rates by varying the total number of collocation points used for spatial discretization and the time steps, validating our*

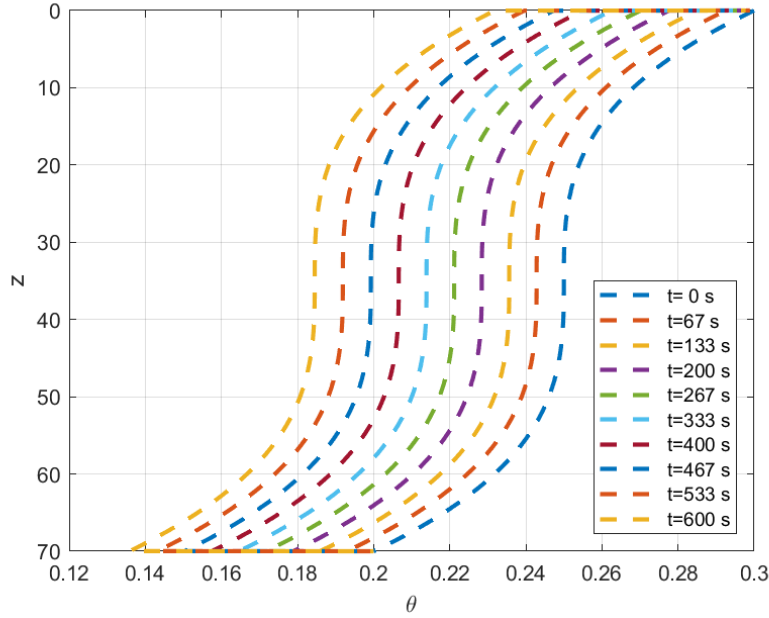


FIGURE 2. Soil moisture profiles at different times, obtained by the proposed method, referred to Example 4.1: the top boundary conditions are represented by a decreasing function, that is simulating a desaturation process.

*theoretical results. We fix the evaluation time and collocation point, and introduce the discrete relative  $L^2$ -error and  $L^1$ -error, for space and time respectively, as follows*

$$E_{L^2}^t = \frac{\sum_{h=0}^N |\theta^N(z_h, t) - \theta^*(z_h, t)|^2}{\sum_{h=0}^N |\theta^N(z_h, t)|^2}, \quad E_{L^1}^z = \frac{\sum_{m=0}^{N_T} |\theta^N(z, t_m) - \theta^*(z, t_m)|}{\sum_{m=0}^{N_T} |\theta^N(z, t_m)|}$$

*where  $\theta^*(z, t)$  denotes the reference solution obtained by our method using a finer spatial mesh. In Table 1 we compute the discrete relative  $L^2$ -error and the convergence rate with respect to the total number of meshpoints used to discretize in space and by fixing the time step. It can be observed that the convergence rate is coherent with the estimate in Theorem 3.4.*

*We also test the numerical order of convergence of the scheme with respect to the time step. The results are reported in Table 2.*

**Example 4.2.** *As already considered by [27], we select a Glendale clay loam, characterized by the following parameters*

$$\theta_r = 0.1060, \theta_S = 0.4686, \alpha = 0.0104, n = 1.3954, K_S = 1.5162e - 4 \text{ cm/s.}$$

*We put neither sink nor source on this simulation. Peridynamic parameter is  $\delta = 0.15$*

$N$	$E_{L^2}^t$	Convergence rate
100	$3.4523 \times 10^{-5}$	—
200	$8.0098 \times 10^{-6}$	2.1077
400	$1.7378 \times 10^{-6}$	2.1562
800	$3.1875 \times 10^{-7}$	2.2481
1600	$3.5384 \times 10^{-8}$	2.4512

TABLE 1. Numerical orders of convergence of the scheme with respect to the total number of collocation points relative to Example 4.1. The parameters for the simulation are  $t = 600$  s and  $\Delta t = 0.06$  s.

$\Delta t$	$E_{L^1}^z$	Convergence rate
0.2	$4.9127 \times 10^{-5}$	—
0.1	$2.4586 \times 10^{-5}$	0.9987
0.05	$1.2309 \times 10^{-5}$	0.9984
0.025	$6.1703 \times 10^{-6}$	0.9977
0.01	$2.4911 \times 10^{-6}$	0.9956

TABLE 2. Numerical orders of convergence of the scheme with respect to the time step relative to Example 4.1. The parameters for the simulation are  $z = 35$  cm and  $N = 3200$ .

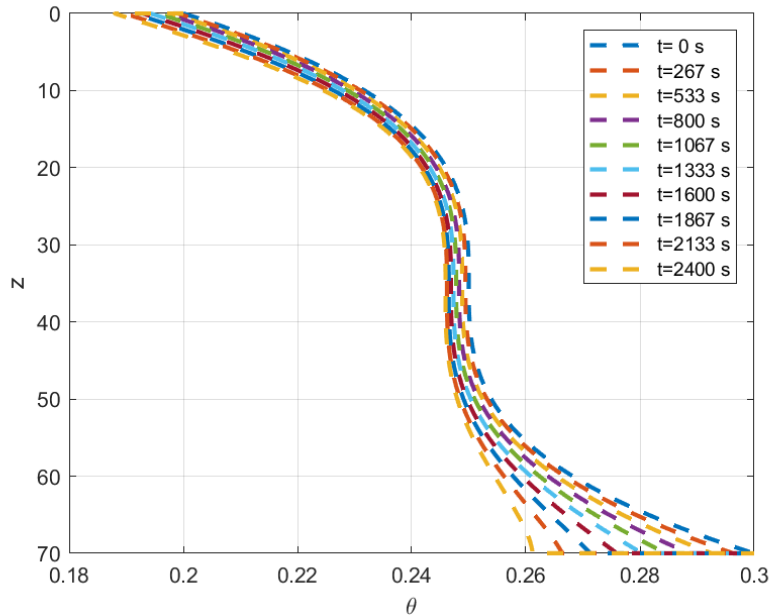


FIGURE 3. Numerical solution relative to Example 4.2.



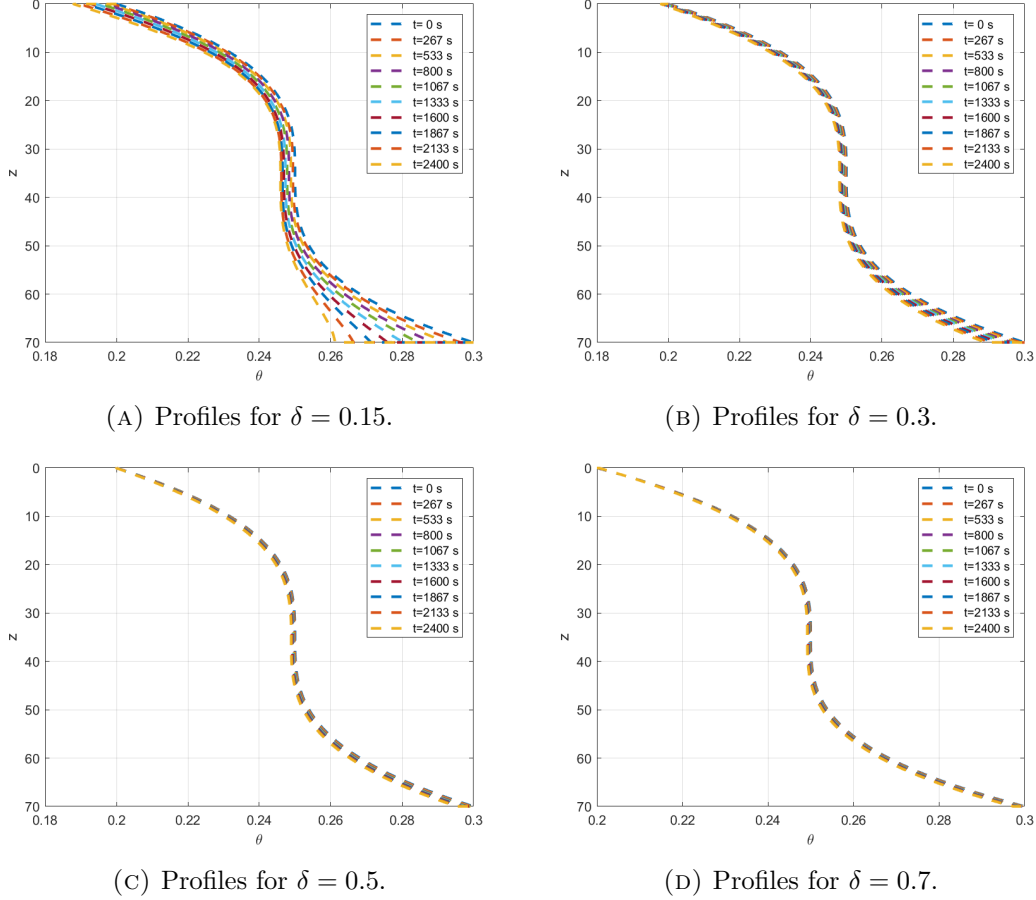


FIGURE 4. Numerical simulations relative to soil and parameters in Example 4.2 for  $\delta \in \{0.15, 0.3, 0.5, 0.7\}$ .

in (2.1). Our boundary conditions are constant with values

$$\begin{aligned} \theta(0, t) &= 0.2, \quad t \in [0, T], \\ \theta(Z, t) &= 0.3, \quad t \in [0, T], \end{aligned}$$

while initial condition follows a nonlinear profile of the form

$$\theta(z, 0) = -0.05z^3 + 0.25, \quad x := \frac{Z - 2z}{Z}, \quad z \in [0, Z].$$

We select  $Z = 70$  cm,  $T = 2400$  s; moreover, we used  $\Delta t = 2.4$  s and  $\Delta x = 0.3$  cm. The resulting water content profiles are shown in Figure 3.

It is worth comparing what happens to the dynamical behavior as a function of the horizon radius  $\delta \in [0, 1]$ . We depict solution profiles in Figure 4 for different values of  $\delta \in \{0.15, 0.3, 0.5, 0.7\}$ . It can be noticed how profile behaviors tend to be more and more nonlocal as  $\delta$  increases approaching 1, as expected.

**Remark 4.3.** *We stress that employing classical influence functions, e.g. uniform or linear as in [29], provides nonphysical solutions in terms of water content. Indeed, within our semi-discretized spectral scheme, the implementation of a classical influence function makes the numerical solution exceeds at some points the non-saturation interval  $[\theta_r, \theta_S]$ .*

## 5. CONCLUSIONS AND FUTURE WORKS

Starting from an appropriate and physically based rewriting of Richards' equation using non-locality theory, we propose to compute its numerical solution using a semi-discretized time forward scheme based on Chebyshev transform. We prove that such approach converges in suitable Sobolev spaces, providing a theoretical background for further extensions of the present work to higher dimensional domains. We also propose a new kind of convolutional kernel, or influence function, in order to manage the peridynamic behavior of the proposed model. Such an influence function distributes its effect on the domain so to correctly catch boundary conditions. In fact, we experienced major benefits from this choice, as numerical convergence turns out to be robust with respect to time, and compared to results coming from classical choices of influence functions. To testify our theoretical analysis, we have performed several experiments, on a wide range on soils, in MATLAB. We have considered different Dirichlet boundary conditions and linear and non-linear initial conditions and show that, with suitable discretization step-sizes, our method is reliable and accurate.

The present work suggests several possible directions for future and already ongoing research studies. For instance, it would be of interest applying Eulerian-Lagrangian methods (e.g. [1]) in the proposed peridynamic framework for Richards' equation, while the idea of introducing a basic control approach on the boundary conditions, as in [8], could be adapted as well. Another development would consider non-local terms in time, so to resort to numerical solvers coming from specific tools in fractional differential calculus (see [25, 23]), or, even more promisingly, by spectral methods in 2D (see [34, 30, 36]).

## ACKNOWLEDGMENTS

All authors are member of the INdAM Research group GNCS.

MB acknowledges the partial support of the 2022 project “Modelli di evoluzione non locali: analisi, trattamento numerico e algoritmi” funded by GNCS-INdAM, INdAM - GNCS 2023 Project, grant number CUP\_E53C22001930001, and the partial support of the CNR project “MENTOR”.

FVD acknowledges the partial support of the 2022 project “Modelli di evoluzione non locali: analisi, trattamento numerico e algoritmi” funded by GNCS-INdAM; he has also been supported by *REFIN* Project, grant number 812E4967 funded by Regione Puglia, and by INdAM-GNCS 2023 Project, grant number CUP\_E53C22001930001.

SFP has been supported by *REFIN* Project, grant number D1AB726C funded by Regione Puglia, by INdAM - GNCS 2023 Project, grant number CUP\_E53C22001930001 and by *PNRR MUR - M4C2*, grant number N00000013 - CUP D93C22000430001. She also acknowledges the partial support of “Finanziamento giovani ricercatori 2022” funded by GNCS-INdAM.

## REFERENCES

- [1] E. Abreu, R. De la cruz, J.C. Juajibioy, and W. Lambert. Lagrangian-Eulerian Approach for Nonlocal Conservation Laws. *Journal of Dynamics and Differential Equations*, 2022.
- [2] B. Aksoylu and A. Kaya. Conditioning and error analysis of nonlocal operators with local boundary conditions. *Journal of Computational and Applied Mathematics*, 335:1–19, 2018.
- [3] T. Arbogast, M.F. Wheeler, and N.Y. Zhang. A Nonlinear Mixed Finite Element Method for a Degenerate Parabolic Equation Arising in Flow in Porous Media. *SIAM Journal on Numerical Analysis*, 33(4):1669—1687, 1996.
- [4] Günter Baszenski and Manfred Tasche. Fast polynomial multiplication and convolutions related to the discrete cosine transform. *Linear Algebra and Its Applications*, 252(1-3):1 – 25, 1997.
- [5] M. Berardi, F. Difonzo, F. Notarnicola, and M. Vurro. A transversal method of lines for the numerical modeling of vertical infiltration into the vadose zone. *Applied Numerical Mathematics*, 135:264 – 275, 2019.
- [6] M. Berardi, F. Difonzo, M. Vurro, and L. Lopez. The 1D Richards’ equation in two layered soils: a Filippov approach to treat discontinuities. *Advances in Water Resources*, 115:264–272, may 2018.
- [7] M. Berardi and G. Girardi. Richards’ equation with non-local root water uptake modeling plant water deficit. submitted, December 2022.
- [8] Marco Berardi, Marcello D’Abbicco, Giovanni Girardi, and Michele Vurro. Optimizing water consumption in Richards’ equation framework with step-wise root water uptake: a simplified model. *Transport in Porous Media*, 142:469–498, 2022.
- [9] Marco Berardi and Fabio V. Difonzo. Strong solutions for Richards’ equation with Cauchy conditions and constant pressure gradient. *Environmental Fluid Mechanics*, 20(1):165–174, Feb 2020.
- [10] Marco Berardi, Fabio Vito Difonzo, and Luciano Lopez. A mixed MoL-TMoL for the numerical solution of the 2D Richards’ equation in layered soils. *Computers & Mathematics with Applications*, 79:1990–2001, 2020.
- [11] Luca Bergamaschi and Mario Putti. Mixed finite elements and newton-type linearizations for the solution of Richards’ equation. *International Journal for Numerical methods in Engineering*, 45:1025–1046, 1999.
- [12] Florin Bobaru and Monchai Duangpanya. A peridynamic formulation for transient heat conduction in bodies with evolving discontinuities. *Journal of Computational Physics*, 231(7):2764–2785, 2012.
- [13] C. Canuto and A. Quarteroni. Approximation results for orthogonal polynomials in Sobolev spaces. *Math. Comp.*, 38:67–86, 1982.
- [14] Andrea Carminati. A model of root water uptake coupled with rhizosphere dynamics. *Vadose Zone Journal*, 11, 2012.
- [15] Jesús Carrera, Xavier Sánchez-Vila, Inmaculada Benet, Agustín Medina, Germán Galarza, and Jordi Guimerà. On matrix diffusion: formulations, solution methods and qualitative effects. *Hydrogeology Journal*, 6:178–190, 1998.
- [16] V. Casulli and P. Zanolli. A Nested Newton-Type Algorithm for Finite Volume Methods Solving Richards’ Equation in Mixed Form. *SIAM Journal on Scientific Computing*, 32(4):2255–2273, 2010.
- [17] Michael A. Celia, Eftimios T. Bouloutas, and Rebecca L. Zarba. A general mass-conservative numerical solution for the unsaturated flow equation. *Water Resources Research*, 26(7):1483–1496, 1990.
- [18] G. M. Coclite, F. Paparella, and S. F. Pellegrino. On a salt fingers model. *Nonlinear Analysis*, 176:100 – 116, 2018.
- [19] Antonio Coppola, Alessandro Comegna, Giovanna Dragonetti, Horst H. Gerke, and Angelo Basile. Simulated preferential water flow and solute transport in shrinking soils. *Vadose Zone Journal*, 14(9):vzj2015.02.0021, 2015.
- [20] Antonio Coppola, Horst H. Gerke, Alessandro Comegna, Angelo Basile, and Vincenzo Comegna. Dual-permeability model for flow in shrinking soil with dominant horizontal deformation. *Water Resources Research*, 48(8), 2012.
- [21] E. Dal Santo, C. Donadello, S. F. Pellegrino, and M. D. Rosini. Representation of capacity drop at a road merge via point constraints in a first order traffic model. *ESAIM: M2AN*, 53(1):1–34, 2019.

- [22] Amir H. Delgoushaie, Daniel W. Meyer, Patrick Jenny, and Hamdi A. Tchelepi. Non-local formulation for multiscale flow in porous media. *Journal of Hydrology*, 531:649–654, 2015.
- [23] F. V. Difonzo and R. Garrappa. A numerical procedure for fractional-time-space differential equations with the spectral fractional Laplacian, 2022. accepted on Springer INdAM Series.
- [24] Fabio V. Difonzo, Costantino Masciopinto, Michele Vurro, and Marco Berardi. Shooting the numerical solution of moisture flow equation with root uptake: a Python tool. *Water Resources Management*, 35:2553–2567, 2021.
- [25] Roberto Garrappa and Marina Popolizio. Generalized exponential time differencing methods for fractional order problems. *Computers & Mathematics with Applications*, 62(3):876–890, 2011. Special Issue on Advances in Fractional Differential Equations II.
- [26] Ivan A. Guerrini and D. Swartzendruber. Soil water diffusivity as explicitly dependent on both time and water content. *Soil Science Society of America Journal*, 56(2):335–340, 1992.
- [27] R. G. Hills, I. Porro, D. B. Hudson, and P. J. Wierenga. Modeling one-dimensional infiltration into very dry soils: 1. model development and evaluation. *Water Resources Research*, 25(6):1259–1269, 1989.
- [28] Rami Jabakhanji. *Peridynamic Modeling of Coupled Mechanical Deformations and Transient Flow in Unsaturated Soils*. PhD thesis, Purdue University, 2013. [https://docs.lib.purdue.edu/open\\_access\\_dissertations/147](https://docs.lib.purdue.edu/open_access_dissertations/147).
- [29] Rami Jabakhanji and Rabi Mohtar. A peridynamic model of flow in porous media. *Advances in Water Resources*, 78, 02 2015.
- [30] S. Jafarzadeh, L. Wang, A. Larios, and F. Bobaru. A fast convolution-based method for peridynamic transient diffusion in arbitrary domains. *Computer Methods in Applied Mechanics and Engineering*, 375:113633, 2021.
- [31] M. L. Kavvas, A. Ercan, and J. Polsinelli. Governing equations of transient soil water flow and soil water flux in multi-dimensional fractional anisotropic media and fractional time. *Hydrology and Earth System Sciences*, 21(3):1547–1557, 2017.
- [32] C.E. Kees, M.W. Farthing, and C.N. Dawson. Locally conservative, stabilized finite element methods for variably saturated flow. *Computer Methods in Applied Mechanics and Engineering*, 197(51):4610–4625, 2008.
- [33] H. Li, M.W. Farthing, and C.T. Miller. Adaptive local discontinuous Galerkin approximation to Richards’ equation. *Advances in Water Resources*, 30(9):1883–1901, 2007.
- [34] L. Lopez and S. F. Pellegrino. A fast-convolution based space–time Chebyshev spectral method for peridynamic models. *Advances in Continuous and Discrete Models*, 70(1), 2022.
- [35] L. Lopez and S. F. Pellegrino. A non-periodic Chebyshev spectral method avoiding penalization techniques for a class of nonlinear peridynamic models. *International Journal for Numerical Methods in Engineering*, 123(20):4859–4876, 2022.
- [36] L. Lopez and S. F. Pellegrino. A space-time discretization of a nonlinear peridynamic model on a 2D lamina. *Computers and Mathematics with Applications*, 116:161–175, 2022.
- [37] Luciano Lopez and Sabrina Francesca Pellegrino. Computation of Eigenvalues for Nonlocal Models by Spectral Methods. *Journal of Peridynamics and Nonlocal Modeling*, 2021.
- [38] Gianmarco Manzini and Stefano Ferraris. Mass-conservative finite volume methods on 2-d unstructured grids for the Richards’ equation. *Advances in Water Resources*, 27(12):1199 – 1215, 2004.
- [39] Costantino Masciopinto and Giuseppe Passarella. Mass-transfer impact on solute mobility in porous media: A new mobile-immobile model. *Journal of Contaminant Hydrology*, 215:21–28, 2018.
- [40] K. Mitra and I.S. Pop. A modified l-scheme to solve nonlinear diffusion problems. *Computers & Mathematics with Applications*, 2018.
- [41] Federico Municchi, Nicodemo Di Pasquale, Marco Dentz, and Matteo Icardi. Heterogeneous multi-rate mass transfer models in openfoam®. *Computer Physics Communications*, 261:107763, 2021.
- [42] Insa Neuweiler, Daniel Erdal, and Marco Dentz. A Non-Local Richards Equation to Model Unsaturated Flow in Highly Heterogeneous Media under Nonequilibrium Pressure Conditions. *Vadose Zone Journal*, 11(3), 08 2012.
- [43] Tao Ni, Francesco Pesavento, Mirco Zaccariotto, Ugo Galvanetto, Qi-Zhi Zhu, and Bernhard A. Schrefler. Hybrid FEM and peridynamic simulation of hydraulic fracture propagation in saturated porous media. *Computer Methods in Applied Mechanics and Engineering*, 366:113101, 2020.

- [44] Yakov Pachepsky, Dennis Timlin, and Walter Rawls. Generalized Richards' equation to simulate water transport in unsaturated soils. *Journal of Hydrology*, 272(1):3–13, 2003.
- [45] S. F. Pellegrino. On the implementation of a finite volumes scheme with monotone transmission conditions for scalar conservation laws on a star-shaped network. *Applied Numerical Mathematics*, 155:181 – 191, 2020.
- [46] I.S. Pop, F. Radu, and P. Knabner. Mixed finite elements for the richards' equation: linearization procedure. *Journal of Computational and Applied Mathematics*, 168(1–2):365 – 373, 2004.
- [47] Stephen L. Rawlins and Walter H. Gardner. A test of the validity of the diffusion equation for unsaturated flow of soil water. *Soil Science Society of America Journal*, 27(5):507–511, 1963.
- [48] M. I. Romashchenko, V. O. Bohaienko, T. V. Matiash, V. P. Kovalchuk, and A. V. Krucheniuk. Numerical simulation of irrigation scheduling using fractional Richards equation. *Irrigation Science*, 39:385–396, 2021.
- [49] Pouria Sheikhabaee, Farshid Mossaiby, and Arman Shojaei. An efficient peridynamic framework based on the arc-length method for fracture modeling of brittle and quasi-brittle problems with snapping instabilities. *Computers & Mathematics with Applications*, 136:165–190, 2023.
- [50] S.A. Silling. Reformulation of elasticity theory for discontinuities and long-range forces. *Journal of the Mechanics and Physics of Solids*, 48(1):175–209, 2000.
- [51] S.A. Silling and R.B. Lehoucq. Peridynamic theory of solid mechanics. In Hassan Aref and Erik van der Giessen, editors, *Advances in Applied Mechanics*, volume 44 of *Advances in Applied Mechanics*, pages 73–168. Elsevier, 2010.
- [52] Xun Wu, Qiang Zuo, Jianchu Shi, Lichun Wang, Xuzhang Xue, and Alon Ben-Gal. Introducing water stress hysteresis to the Feddes empirical macroscopic root water uptake model. *Agricultural Water Management*, 240:106293, 2020.
- [53] Huaxiang Yan, Majid Sedighi, and Andrey P. Jivkov. Peridynamics modelling of coupled water flow and chemical transport in unsaturated porous media. *Journal of Hydrology*, 591:125648, 2020.
- [54] K. Zhou and Q. Du. Mathematical and numerical analysis of linear peridynamic models with nonlocal boundary conditions. *SIAM Journal on Numerical Analysis*, 48(5):1759–1780, 2010.
- [55] Jiří Šimůnek and Martinus Th. van Genuchten. Contaminant transport in the unsaturated zone: Theory and modeling. In J.H. Cushman and D.M Tartakovsky, editors, *The Handbook of Groundwater Engineering*, chapter 8, pages 266–290. CRC Press, Boca Raton, 2016.

ISTITUTO DI RICERCA SULLE ACQUE, CONSIGLIO NAZIONALE DELLE RICERCHE, VIA F. DE BLASIO  
5, 70132 BARI, ITALY

*Email address:* marco.berardi@ba.irsra.cnr.it

DIPARTIMENTO DI MATEMATICA, UNIVERSITÀ DEGLI STUDI DI BARI ALDO MORO, VIA E. ORABONA  
4, 70125 BARI, ITALY

*Email address:* fabio.difonzo@uniba.it

DIPARTIMENTO DI INGEGNERIA ELETTRICA E DELL'INFORMAZIONE, POLITECNICO DI BARI, VIA E.  
ORABONA 4, 70125 BARI, ITALY

*Email address:* sabrinafrancesca.pellegrino@poliba.it